JOURNAL OF SOLID STATE CHEMISTRY 91, 286–295 (1991)

Theoretical Estimation of Overlapping Repulsive Energies, Polarizabilities, and Lattice Energy in WO_3

E. IGUCHI, H. SUGIMOTO, A. TAMENORI, AND H. MIYAGI

Materials Science, Department of Mechanical Engineering and Materials Science, Faculty of Engineering, Yokohama National University, Tokiwadai, Hodogaya-Ku, Yokohama, 240 Japan

Received August 27, 1990; revised November 14, 1990

Repulsive energies resulting from overlap of $W^{6+}-W^{6+}$, $W^{6+}-O^{2-}$, and $O^{2-}-O^{2-}$ pairs were calculated within the framework of the free ion model constructed by Wedepohl. Polarizabilities of ions in the monoclinic structure of WO_3 were obtained following the theoretical treatments of Parker. Using these values, the lattice energy (cohesive energy) of the monoclinic structure of WO_3, consisting of the long range coulombic interaction energy, the repulsive energy, van der Waals interaction energy, and the zero point energy, was evaluated to be -235.53 eV per WO_3 formula unit and compared with the experimental value determined by the Born–Haber cycle analysis, $-(239.23 \sim 243.44)$ eV per WO_3 formula unit, with a discrepancy of 3%. In comparison with other oxides, van der Waals interactions are found to contribute remarkably to the lattice energy in WO_3. The lattice energy in the ε-phase at low temperatures was also calculated, using the same parameters employed in the calculation of the lattice energy in the monoclinic structure. The lattice energy in the ε-phase is -235.60 eV per WO_3 formula unit which is found to be in good agreement with the experimental value. In the ε-phase, the contribution of van der Waals interactions plays also an important role in the lattice energy as well as the monoclinic structure.

1. Introduction

Not only the structures of WO_3 correlated with phase transitions and formation of crystallographic shear (*CS*) planes (*1–3*) but also the physical properties associated with polarons formed in WO_3 are of great interest (*4–6*). Experimental results on these investigations are now available in detail, but these experiments require rigorous interpretations based upon reliable theoretical criteria. In fact, the dynamic properties of *CS* planes formed in WO_3 and their microstructures, observed in electron microscopic and X-ray measurements, are analyzed quantitatively, using strain energy calculations (*1–3, 7–10*). There are good correlations between the theoretical predictions made by strain energy calculations and the experimental results. Sometimes, however, these calculations are too simple to account for more essential problems with *CS* planes and also with electronic behaviors of a polaron associated with a local lattice distortion. They require more sophisticated theoretical treatments (*11, 12*). The shell model which we have employed frequently (*11–13*) is surely one of the candidates for such treatments. In fact, the shell model reveals that the lattice relaxation due

0022-4596/91 $3.00

to the electronic polarizability of oxygen ions plays a very significant role in the formation of *CS* planes (*13*). Furthermore, the combination of the shell model and Anderson's attractive potential (*14*) enables us to describe the polaron behaviors theoretically in the Ti–O binary system (*15*). One should remember, here, that the shell model starts, first, with the calculation of the lattice energy (i.e., cohesive energy) of a perfect crystal, consisting of the long range coulombic interaction energies, the short range overlapping repulsive energies, and the van der Waals interaction energies. In spite of a rather simple treatment in evaluating the coulombic interaction energies (Madelung energies) (*16, 17*), the overlapping repulsive energies between ions are determined empirically (*11, 12, 18*), in general using the experimental values for compressibility, bulk modulus, elastic constants, force constants, and lattice energy which are not yet available in WO_3 because of the apparent difficulties in growing single crystals large enough for measuring these properties. In addition, the expression for van der Waals energies contains electronic polarizabilities and approximate average excitation energies of ions (*19*), which have not been yet obtained experimentally. Thus, theoretical estimation of the lattice energy in WO_3 looks difficult and, consequently, quantitative interpretations of the behaviors of *CS* planes and polarons in this material are postponed, unfortunately, in comparison with the Ti–O binary system. However, the development of the theoretical treatments now enables us to calculate the repulsive and van der Waals energies in WO_3 without experimental data. In this report, we calculate overlapping repulsive energies, polarizabilities of ions, van der Waals energies in the monoclinic structure of WO_3 at the room temperature, and, finally, the lattice energy in this structure. Although we previously calculated polarizabilities for WO_3 (*20*), our calculations contained theoretical errors and wrong values were presented. Therefore, we have carried out the recalculation on polarizabilities in this report.

TABLE I

ION POSITIONS IN THE MONOCLINIC STRUCTURE OF WO_3

Ions	x	y	z
$W^{6+}(1)$	0.2465	0.0269	0.2859
$W^{6+}(2)$	0.2538	0.0353	0.7807
$O^{2-}x1$	0.0025	0.0350	0.2106
$O^{2-}x2$	0.9974	0.4636	0.2161
$O^{2-}y1$	0.2840	0.2605	0.2848
$O^{2-}y2$	0.2099	0.2568	0.7318
$O^{2-}z1$	0.2827	0.0383	0.0046
$O^{2-}z2$	0.2856	0.4840	0.9944

Once the physical parameters relevant to repulsive interactions between ions and polarizabilities are available, they would be very helpful in understanding the essential behaviors of *CS* planes and polarons which the strain energy calculations cannot explain.

2. Theoretical Treatment and Results

2. 1. *Crystal Structures*

WO_3 has several structures correlated with phase transitions (*1*). Though there are several reports on the monoclinic structure at room temperature (*21–23*), we have referred to the results obtained by Loopstra *et al.* (*24*), using the neutron diffraction method, with the lattice parameters, a_0 = 0.7306 nm, b_0 = 0.7540 nm, c_0 = 0.7692 nm, and β = 90.88°. All ions are in general positions as presented in Table I.

2. 2. *Overlapping Repulsive Energies between Ions*

Repulsive interactions between ions are generally approximated by some variation of the Born–Mayer potential, Aexp(-Br),

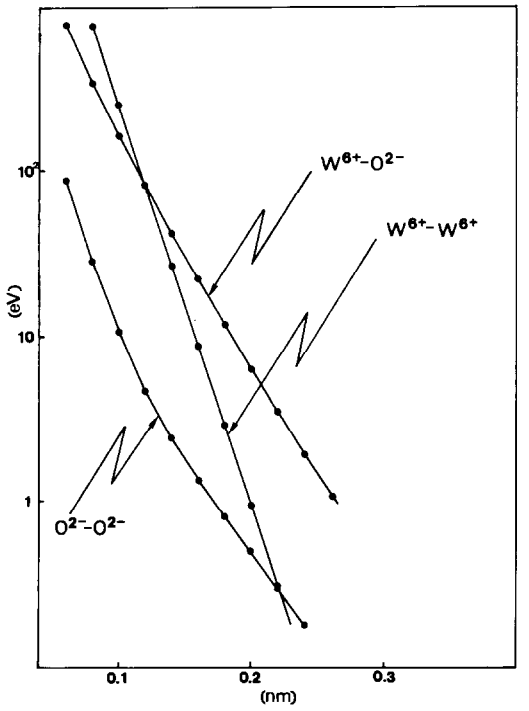

FIG. 1. The repulsive energy (eV) of each ion pair in WO_3 as a function of the interionic spacing (nm).

the parameters of which, A and B, are determined from perfect crystal properties. As described in the introduction, however, these properties are not yet available for WO_3. Alternatively, we calculated the repulsive energies within the framework of the free ion model constructed by Wedepohl (*25–27*) as we did in our previous reports (*28, 29*). Each ion is assumed to consist of a spherical negative charge distribution of electrons. To determine the charge distribution, the Hartree–Fock wave functions obtained by Watson for O^{2-} (*30*) and that of the W ion calculated using the short Hermann–Skillman programs (*31*) were used. The charge distribution of every ion pair can be truncated without serious errors at the truncated radius of O^{2-} ions, 0.344 nm, which was estimated by the procedure of

TABLE II

THE BORN–MAYER PARAMETERS DETERMINED FROM A SEGMENTED FIT TO THE REPULSIVE ENERGIES OF THE ION PAIRS

Ion pair	A(eV)	B(nm^{-1})	Range of separation (nm)
W^{6+}–W^{6+}	1.008×10^5	61.22	$r < 0.08$
	6.480×10^4	55.70	$r \geqq 0.08$
W^{6+}–O^{2-}	6.497×10^3	37.00	$r < 0.10$
	4.934×10^3	34.25	$0.10 \leqq r < 0.12$
	4.239×10^3	32.98	$0.12 \leqq r < 0.14$
	3.799×10^3	32.20	$0.14 \leqq r < 0.16$
	3.404×10^3	31.51	$0.16 \leqq r < 0.18$
	3.020×10^3	30.85	$0.18 \leqq r < 0.20$
	2.403×10^3	29.71	$0.20 \leqq r < 0.22$
	2.633×10^3	30.09	$0.22 \leqq r$

Hartree–Hartree (*32*). In Fig. 1, are shown repulsive energies of ion pairs as a function of the interionic spacing.

The Born–Mayer parameters, A and B, appropriate to the ion pairs, W^{6+}–W^{6+} and W^{6+}–O^{2-}, and the designated range of separation were obtained by fitting the numerical results in Fig. 1 and are tabulated in Table II. As for the O^{2-}–O^{2-} pair, the Born–Mayer parameters are given in our previous report (*29*).[1]

2. 3. *Polarizabilities*

Polarizabilities of ions in a crystal are required in the calculations of lattice energies in a perfect crystal and a crystal containing imperfections such as lattice defects or polarons. Parker proposed a theoretical method for estimating polarizabilities in a crystal (*34*). Taking Lorentz factors into account, she constructed simultaneous nonlinear scalar equations of electric fields acting on lattice points which include unknowns

[1] Though it is described in Ref. [29] that the Born-Mayer constants of the O^{2-}–O^{2-} pair were determined with the wave function of Clementi and Roetti for O^{2-} (*33*), the wave function calculated by Watson (*30*) was used actually.

such as polarizabilities and ratios of internal fields acting on lattices to the applied field. Then, we can estimate polarizabilities if the number of unknowns is less than that of scalar equations. We have calculated the Lorentz factors in the monoclinic structure and found that the *xy*, *yz*, and *zx* components of the Lorentz factor at each lattice site are not zero, although their values are very small compared with *xx*, *yy*, and *zz* components. In such a case, the number of the unknowns exceeds that of equations, unfortunately. In order to overcome this difficulty, we reconstructed an appropriately modified crystal structure as well as our previous calculation (*20*) in which, however, we found serious errors in the theoretical treatments and wrong values were presented for polarizabilities. Then we recalculated approximate polarizabilities in the unit cell with the lattice parameters, $a = a_0/2$, $b = b_0/2$, $c = c_0/2$, and $\beta = 90.88°$. Sites 1 at (0,0,0) are occupied by W^{6+} ions, while O^{2-} ions occupy sites 2 at (1/2,0,0), 3 at (0,1/2,0), and 4 at (0,0,1/2). These sites in this unit cell are numbered for the usage *only in this section (2. 3)*. The local electric field, E_i, acting on a particular site in the *i*th lattice is,

$$E_i = E_0 + \sum_{j=1}^{4} P_j F_{ij}, \qquad (1)$$

where E_0 and P_j denote the applied field and the polarization of an ion in the *j*th lattice. F_{ij} is the Lorentz factor for the dipole–dipole interaction between the lattices, *i* and *j*, which has the form of the second-rank tensor as follows,

$$F_{ij} = 4\pi I/3 + V\Sigma'_j(3\mathbf{r}_{in}\mathbf{r}_{in} - \mathbf{r}_{in}{}^2 I)/\mathbf{r}_{in}{}^5, \qquad (2)$$

where I is the 3×3 unit matrix, $\mathbf{r}_{in}$ is the vector from the *j*th lattice in the *n*th unit cell to the *i*th lattice in the first unit cell, $\mathbf{r}_{in}\mathbf{r}_{in}$ represents the dyadic product of $\mathbf{r}_{in}$, Σ'_j signifies the summation of the contributions of the *j*th lattice in each cell to the *i*th lattice in the first unit cell with the volume V. In Table III, each component of F_{ij} evaluated using Eq. (3) is tabulated, where $F_{ij} = F_{ji}$.

TABLE III

COMPONENTS OF THE LORENTZ FACTORS IN THE MONOCLINIC STRUCTURE OF WO_3

	xx	*yy*	*zz*	*xy*	*zx*	*yz*
f_{11}	4.530	4.136	3.901	0.0	−0.058	0.0
f_{12}	36.872	−12.082	−12.224	0.0	−0.006	0.0
f_{13}	−10.512	33.934	−10.856	0.0	−0.051	0.0
f_{14}	−9.722	−9.930	32.218	0.0	−0.631	0.0
f_{22}	4.530	4.136	3.901	0.0	−0.058	0.0
f_{23}	8.091	9.295	−4.820	0.0	−0.013	0.0
f_{24}	7.576	−4.521	9.511	0.0	0.374	0.0
f_{33}	4.530	4.136	3.901	0.0	−0.058	0.0
f_{34}	−4.111	7.979	8.699	0.0	−0.194	0.0
f_{44}	4.530	4.136	3.901	0.0	−0.058	0.0

When the frequency of the driving field is sufficiently high, only electronic polarization is effective (optical case). In addition to Eq. (2), there is another useful relation between the total polarization and the refractive indices,

$$(n_x^2\mathbf{i} + n_y^2\mathbf{j} + n_z^2\mathbf{k})E_0 = E_0 + 4\pi\Sigma_j P_j, \qquad (3)$$

where n_x, n_y, and n_z indicate x, y, and z components of the refractive index and **i, j,** and **k** are the unit vectors along the x, y, and z axes. Using the refractive indices obtained by Salje (*35*), i.e., $n_x^2 = 7.306$, $n_y^2 = 5.645$, and $n_z^2 = 5.212$, Eqs. (1) and (3) enable us to evaluate the electronic polarizability of the O^{2-} ion in WO_3. The electronic polarizability of ions in the *j*th lattice (α_j^e) is defined by $P_j = (\alpha_j^e)E_j/V$. Making use of the ratios $X_{jk} = E_{jk}/E_{0k}$, the following scalar equations along the *k*th direction ($k = x$, y, or z) can be obtained from Eqs. (1) and (3).

$$X_{ik} = 1 + \sum_{j=1}^{4} (\alpha_j^e)_k F_{ij} X_{jk}/V \quad i = 1\text{–}4 \qquad (4)$$

$$n_k^2 = 1 + 4\pi \sum_{j=1}^{4} (\alpha_j^e)_k X_{jk}/V. \qquad (5)$$

Here we have assumed that the O^{2-} ions at every site have the same value of electronic

polarizability, i.e., $(\alpha_j^e) = (\alpha_{O^{2-}}^e)_k$ $(i = 2\text{–}4)$, as in Parker's treatment and our previous calculation (*20*). For the electronic polarizability of the W^{6+} ion, we employed the value calculated previously, using Ruffa's argument for electronic polarizabilities of cations in crystals (*36, 37*), i.e., $\alpha_{W^{6+}}^e = 1.091 \times 10^{-3}$ nm^3, under the assumption that the electronic polarizability of the W^{6+} ion is isotropic in WO_3. Then, we can evaluate the electronic polarizabilities of the O^{2-} ions in each direction. The results calculated by the Brent method are listed in Table IV.

When the driving frequency is low (static case), there are additional ionic polarization terms in the local fields. Instead of Eqs. (4) and (5), the following equations apply to the static case in the applied field.

$$X_{ik} = 1 + \left\{ [(\alpha_{W^{6+}}^e) + (\alpha_{W^{6+}}^i)_k] X_{lk} + [(\alpha_{O^{2-}}^e)_k + (\alpha_{O^{2-}}^i)_k] \left(\sum_{j=2}^{4} X_{jk} F_{ij} \right) - (\alpha^i)_k (X_{ik}/q_i) \sum_{j=1}^{4} F_{ij} q_j \right\} / V \qquad i = 1\text{–}4 \quad (6)$$

$$\varepsilon_{0k} = 1 + 4\pi \left\{ [(\alpha_{W^{6+}}^e) + (\alpha_{W^{6+}}^i)_k] X_{lk} + [(\alpha_{O^{2-}}^e)_k + (\alpha_{O^{2-}}^i)_k] \left(\sum_{j=2}^{4} X_{jk} \right) \right\}, \quad (7)$$

where $(\alpha^i)_k$ represents the ionic polarizability of the ion in the ith lattice. Even if the ionic polarizabilities of ions are assumed to be isotropic and we convert the numerical values for the electronic polarizabilities obtained above, the number of unknowns involved in Eqs. (6) and (7) in each direction is larger than the number of equations. In our previous work (*20*), we used the same assumption as that employed by Parker (*34*), that is, the ionic polarization is assumed either to be a displacement of the tungsten lattices with respect to the oxygen lattices, with the oxygen lattices held fixed, or to be a displacement of the oxygen ions with respect to the fixed tungsten lattices. Using this assumption, it looks possible to evaluate the values for the ionic polarizabilities of the W^{6+} and O^{2-} ions, respectively, because the number of unknowns reduces to that of the equations. However, we will find that Eqs. (6) and (7) never hold if the numerical values calculated in this way are substituted simultaneously for the ionic polarizabilities of O^{2-} and W^{6+} in these equations because they were estimated independently. Therefore, our previous treatment was wrong. Alternatively, for the ionic polarizability of the O^{2-} ion in WO_3, we employed the value of that in $BaTiO_3$, i.e., $\alpha_{O^{2-}}{}^i = 0.378 \times 10^{-3}$ nm^3 (*38*). Then, the number of unknowns reduces to that of the equations. In such a calculation, the static dielectric constant ε_0 determined experimentally is required. Unfortunately, there are no experimental results which are reliable. WO_3 crystals as prepared are generally deficient in oxygen and they contain elec-

TABLE IV

POLARIZABILITIES OF IONS AND VAN DER WAALS CONSTANTS OF THE ION PAIRS IN WO_3

Free ion polarizabilities ($\times 10^{-3}$ nm^3)
$\alpha_{W^{6+}}^f = 0.355$, $\alpha_{O^{2-}}^f = 3.880$
Electronic polarizabilities ($\times 10^{-3}$ nm^3)
$\alpha_{W^{6+}}^e = 1.091$
$\alpha_{O^{2-}}^e$(a) = 6.012, $\alpha_{O^{2-}}^e$(b) = 5.975,
$\alpha_{O^{2-}}^e$(c) = 6.193, $(\alpha_{O^{2-}}^e)_{av} = 6.060$
Ionic polarizabilities ($\times 10^{-3}$ nm^3)
$\alpha_{W^{6+}}^i$(a) = 2.695, $\alpha_{W^{6+}}^i$(b) = 1.507,
$\alpha_{W^{6+}}^i$(c) = 1.276, $(\alpha_{W^{6+}}^i)_{av} = 1.826$
$\alpha_{O^{2-}}^i = 0.378$
Van der Waals constants ($\times 10^{-6}$ eV nm^6)
$C_{W^{6+}\text{–}W^{6+}} = 104.39$
$C_{W^{6+}\text{–}O^{2-}} = 74.24$
$C_{O^{2-}\text{–}O^{2-}} = 220.33$

tronic charge carriers which result in high values of the static dielectric constant because of their polaronic effects. In the present calculation, therefore, we employed the static dielectric constant of doped crystal of WO_3 in which the carriers are trapped, i.e., $\varepsilon_0 = 12$ (*35*). The ionic polarizabilities obtained are listed in Table IV.

2. 4. *van der Waals Constants*

The van der Waals constant between ions i and j, C_{ij}, has the form,

$$C_{ij} = (3/2)(\alpha_i^e)(\alpha_j^e)E_iE_j/(E_i + E_j), \quad (8)$$

where α_i^e and E_i represent the electronic polarizability and some approximate average excitation energy of the ion i, respectively. Though there are several treatments for estimating values of E (*39–41*), we have employed the method proposed by Cantor (*41*). Van der Waals constants were evaluated by equating E for W^{6+} with the 7th ionization potential of the parent W atom, I_7, assigning the value of 8 eV as the ionization potential of the O ion as did Cantor (*41*), and using the electronic polarizabilities of W^{6+} and the average value for the electronic polarizabilities of O ions along the a, b, and c axes which are tabulated in Table IV. Though there are no experimental results on the series of the ionization potentials of the W atom, Rychkov calculated these potential energies theoretically (*42*). We have quoted his results, i.e., $I_7 = 117$ eV. The calculated values for van der Waals constants are tabulated in Table IV.

2. 5. *Lattice Energies*

Based upon an ionic model, the lattice energy (cohesive energy) per WO_3 formula unit, E_L, has the form,

$$\begin{aligned} E_L = (1/2N_0)\Sigma'_i\{&q_i\phi_i(0) \\ &+ \Sigma_{j\neq i}[A_{ij}\exp(-B_{ij}r_{ij}) \\ &+ C_{ij}/r_{ij}^6]\} \\ &+ 9nk_B\theta_D/8 \end{aligned} \quad (9)$$

The first term in the right hand side represents the long range coulombic interaction energy (Madelung energy) that is obtained by using the self potential $\phi(0)$ of each ion which is developed from Ewald's method (*16*) by van Gool and Piken (*17*), where $q_i\phi_i(0)$ indicates the Madelung energy of the ith ion with charge q_i. The second term, $\Sigma_{j\neq i}A_{ij}\exp(-B_{ij}r_{ij})$, is the overlapping repulsive energy of the ith ion, which interacts with other ions in the crystal, where $\Sigma_{j\neq i}$ denotes the summation of interactions of the ith ion with other ions in the crystal and r_{ij} is the interionic spacing between ions, i and j. The Born–Mayer parameters A and B for each particular ion pair are summarized in Table II. The third term is the van der Waals energy including the van der Waals constant C (see Table IV). The last term abbreviates the zero point energy which is calculated as in Wackman *et al.* (*43*), where n is the number of ions per formula unit, k_B and θ_D represent Boltzmann's constant and Debye temperature, respectively. Belovo *et al.* (*44*) reported a value of (380 ± 15) K for the Debye temperature in WO_3. Their result yields a magnitude of 0.147 eV for the zero point energy. In Eq. (9), the numerical factor (1/2) comes in because all pairwise interactions are counted twice and Σ'_i represents the summation of interactions of all ions in the unit cell containing N_0 "molecules" of WO_3. Table V summarizes the Madelung energy, the repulsive energy, the van der Waals energy, and the potential energy of each ion in the monoclinic structure. The total of these contributions yields a calculated lattice energy of −235.53 eV per formula unit.

3. Discussion

As shown in Table V, all W^{6+} ions have nearly the same potential energy, the difference being only 0.5 eV, while those of O^{2-} ions lie in a rather wide range of −47.970 eV to −45.224 eV. The most unstable one

TABLE V

MADELUNG ENERGY (E_M), REPULSIVE ENERGY (E_R), VAN DER WAALS ENERGY (E_W), AND POTENTIAL ENERGY OF EACH ION IN THE MONOCLINIC STRUCTURE OF WO_3

Ions	E_M (eV)	E_R (eV)	E_W (eV)	Potential energy (eV)
$W^{6+}(1)$	−372.56	52.59	−10.54	−330.51
$W^{6+}(2)$	−374.66	54.50	−10.94	−331.10
$O^{2-}x1$	−55.36	17.75	−9.42	−47.03
$O^{2-}x2$	−57.00	18.49	−9.46	−47.97
$O^{2-}y1$	−55.19	17.96	−9.27	−46.50
$O^{2-}y2$	−56.24	19.35	−9.62	−46.51
$O^{2-}z1$	−54.70	18.91	−9.44	−45.23
$O^{2-}z2$	−56.12	18.78	−9.33	−46.67

is O_{z1} at (0.2827, 0.0383, 0.0046). Consequently, this oxygen ion is likely to be eliminated preferentially if an oxygen vacancy is formed. Table V shows a remarkable contribution of the van der Waals interactions which is found to be very large if compared with other oxides (*11, 12, 45*). This is mainly due to a high ionization potential associated with the large valence of cations and also due to large electronic polarizabilities of O^{2-} ions. These values are relatively larger in WO_3 than other oxides.

The lattice energy calculated in this way is compared with the experimental value determined by Born–Haber cycle analysis (*43, 46*). In this cycle, we have to consider all the steps involved in transforming for a tungsten metal atom and oxygen gas atoms to one WO_3 "molecule," that is,

$$E_L = \Delta H_0 - L - (3/2)D_0 + 3A - I, \quad (10)$$

where ΔH_0 is the heat of the formation of WO_3 per molecule, −8.72 eV (*47*), L is the heat of vaporization of the W atom, 8.914 eV (*48*), D_0 is the dissociation energy of the O_2 gas, 5.12 eV (*49*) or 5.09 eV (*50*), A is the affinity of the oxygen atom for two electrons −(6.38~7.77) eV (*51–53*) and I is the sum of the first six ionization potentials of the W atom, 194.82 eV (*42*). Then we have the experimental value of −(239.23~243.44) eV for the lattice energy per WO_3 formula unit compared with the theoretical one, a discrepancy of 3%.

According to Shannon and Prewitt (*54*), the ionic radius of the W^{6+} ion with the configuration number of 6 is 0.060 nm. Such a W^{6+} corresponds to the one at the center of an O^{2-} octahedron. When the configuration number is 4, the ionic radius of W^{6+} is 0.042 nm. O^{2-} ions have a value of 0.140 nm for the ionic radius. In an ionic crystal, it is well known that the interionic spacing in a cation–anion pair is nearly equal to the summation of ionic radii of these ions. If WO_3 crystals contain a rather strong ionic bonding, the interionic distance between W^{6+} and O^{2-} is expected to be about 0.2 nm. In Table VI we have tabulated interionic spacings obtained experimentally (*24*) and found a remarkably wide range of interionic distances between W^{6+} and O^{2-}, 0.1732~0.2116 nm, with an average value of 0.1930 nm, somewhat smaller than the value extrapolated from the ionic radii. It is very interesting that the W^{6+} ion is displaced from the midpoint to one oxygen site in each O–W–O unit, except O_{x1}–W(1)–O_{x2} and

TABLE VI

INTERIONIC DISTANCES OF W^{6+}-O^{2-} IN THE ε-PHASE OF WO_3

	$W^{6+}(1)$	$W^{6+}(2)$
$O^{2-}x1$	0.1867	0.1948
$O^{2-}x2$	0.1931	0.1855
$O^{2-}y1$	0.1783	
$O^{2-}y1$	0.2092	
$O^{2-}y2$		0.1741
$O^{2-}y2$		0.2119
$O^{2-}z1$	0.2186	0.1732
$O^{2-}z2$	0.1740	0.2166

O_{x1}–W(2)–O_{x2}. This fact suggests a rather complicated bonding nature between W^{6+} and O^{2-} and the asymmetry of tungsten positions could be one of the dominant reasons responsible for the considerably larger contribution of van der Waals interactions to the bonding in WO_3. Since interionic spacings in the W^{6+}–O^{2-} bonds are smaller than the value estimated from ionic radii, larger repulsive energies are produced, but, as seen in Table V, the van der Waals contribution cancels out this effect. The balance of these contributions results in a good agreement between the theoretical lattice energy and the experimental one.

Difficulties in determining physical parameters required in the energy calculations on WO_3 have been delaying the progress of these calculations. Despite this, Cormack *et al.* (*55*) and Newtone-Howes *et al.* (*56*) tried the energy calculations of stabilities of WO_3–related structures. Their calculations are, therefore, worth considering. However, the pair potentials employed in their calculations are quite different from ours. As for the potential between W^{6+} and O^{2-}, which is the most important one, the repulsive energy evaluated by substituting the average distance between these ions, 0.1930 nm, for the interionic spacing in their repulsive potential is nearly equal to ours, in spite of remarkable differences in Born–Mayer parameters. The most serious difference in this potential is that they omitted the van der Waals contribution, which plays an important role in the lattice energy of this crystal. Unfortunately, Cormack *et al.* (*55*) did not obtain the lattice energy of WO_3 using their own potentials.

As described several times, theoretical interpretations on the conduction due to a hopping process of polarons, using shell models, are required in order to understand the essential behaviors of polarons formed in WO_3 and the physical parameters obtained here are necessary in shell model calculations. Since the dynamic motions of polarons appear directly in dielectric behaviors and dc resistivities temperatures below about 200 K, we have to treat the energitics of the ε-phase. However, there is no literature on the crystal structure of the ε-phase, except one report by Salje (*57*). Even this report cannot provide the detailed ion positions without an assumption, although the lattice parameters are determined precisely. The ε-phase determined by Salje (*57*) has the monoclinic space group *Pc* with the lattice parameters, $a_0 = 0.5275$ nm, $b_0 = 0.5155$ nm, $c_0 = 0.7672$ nm, and $\beta = 91.7°$. The W positions which Salje presents are

W(1)	(0.00, −0.03, 0.69)
W(2)	(0.00, 0.03, 0.19)
W(3)	(0.50, 0.47, 0.75)
W(4)	(0.50, 0.53, 0.25)

The O positions which we have estimated from his experimental results on the W–O distances and the angle between W–O bondings, under the assumption that the zigzag chain of W(1)–O–W(2) is on (100) and that of W(3)–O–W(4) on the (200) plane, are

O(1)	$(1/2, 1/2 - \delta, 1/2 + \mu)$
O(2)	$(1/2, 1/2 + \delta, \mu)$
O(3~6)	$(\pm 1/4, 0.53 \pm 1/4, 0.22)$
O(7~10)	$(\pm 1/4, 0.47 \pm 1/4, 0.72)$
O(11)	$(0.00, 0.00 - \delta, -0.06 - \mu)$
O(12)	$(0.00, 0.00 + \delta, 0.44 - \mu)$

where $\delta = -0.1477$ and $\mu = 0.0405$.

Using the same values for the physical parameters employed in the calculation of the lattice energy in the monoclinic structure, we have evaluated the Madelung, repulsive, van der Waals, and potential energies of each ion in the ε-phase and tabulated them in Table VII. The sum of the potential energies of ions in a unit cell and the zero point energy yields a value of −235.60 eV for the lattice energy of the ε-phase per WO_3 molecule, which is found to be almost the same as that in the monoclinic structure at

TABLE VII

MADELUNG ENERGY (E_M), REPULSIVE ENERGY (E_R), VAN DER WAALS ENERGY (E_W), AND POTENTIAL ENERGY OF EACH ION IN THE ε-PHASE OF WO_3

Ions	E_M (eV)	E_R (eV)	E_W (eV)	Potential energy (eV)
W^{6+}(1–4)	−373.80	52.11	−10.41	−332.10
O^{2-}(1,2,11,12)	−43.15	14.28	−14.30	−43.17
O^{2-}(3,5,7,9)	−56.19	21.03	−12.69	−47.84
O^{2-}(4,6,8,10)	−55.08	20.52	−13.24	−47.79

room temperature, being in very good agreement with the experimental value. In addition, our calculation reveals that every W ion is equivalent, while there are three groups of equivalent O ions, the first group consisting of O(1), O(2), O(11) and O(12), the second of O(3), O(5), O(7) and O(9), and the third of O(4), O(6), O(8) and O(10). These equivalences are not so easy to find from the crystallographic considerations in such a distorted structure with a low point symmetry.

In the ε-phase, each W ion is located at a position slightly displaced from the center of an O^{2-} octahedron, which is more distorted than that in the monoclinic structure. The four W–O bondings on a plane parallel to (001) in an octahedron have the same distances, i.e., 0.185 nm. On the other hand, the W ions in the zig-zag O–W–O chains along the *c*-axis displace from the middle to one oxygen site, resulting in a remarkable asymmetry in the distances of W–O bondings on the zig-zag chain, i.e., 0.185 and 0.231 nm. This is in common with the monoclinic structure as described before. This fact indicates a rather complicated bonding nature in the ε-phase as well as the monoclinic structure.

Comparison of the results in Table VII with those in Table V indicates the following general features. Each energy term for W ions in the ε-phase has a value nearly equal to that in the monoclinic structure. Among O^{2-} ions in the ε-phase, those in the first group, O(1), O(2), O(11), and O(12), have a considerably high Madelung energy but their repulsive energy is rather low. However, the O^{2-} ions in this group are less stable than not only other groups in this structure but also the most unstable O^{2-} ion in the monoclinic structure, i.e., O_{z1}. Nevertheless, the O^{2-} ions in this group contain the largest contributions from van der Waals interactions. The repulsive energies of O^{2-} ions in other groups of the ε-phase are larger than those in the monoclinic structure. This is mainly because of the short W^{6+}–O^{2-} distances, 0.185 nm, in the ε-phase compared with 0.193 nm, on average, in the monoclinic structure. Alternatively, the van der Waals contributions from O^{2-} ions in these groups are large. Because of the van der Waals energies of these O^{2-} ions, consequently, there is a good agreement between the lattice energy of the ε-phase of WO_3 and the experimental value. These facts described above are indicative of a very significant role of the van der Waals interactions in the ε-phase as well as the monoclinic structure.

Acknowledgments

The authors are very grateful to Dr. E. Salje and Prof. R. J. D. Tilley for helpful suggestions and advice on this work. This research project was supported, in part, by the foundation of Sumitomo Metal Industries Ltd.

References

1. E. IGUCHI AND R. J. D. TILLEY, *Philos. Trans. R. Soc. Lond. A* **289,** 55 (1977).
2. E. IGUCHI AND R. J. D. TILLEY, *J. Solid State Chem.* **24,** 131 (1978).
3. E. IGUCHI AND R. J. D. TILLEY, *J. Solid State Chem.* **32,** 221 (1980).
4. E. SALJE AND G. HOPPMAN, *Philos. Mag. B* **43,** 105 (1981).
5. E. IGUCHI, E. SALJE, AND R. J. D. TILLEY, *J. Solid State Chem.* **38,** 342 (1981).
6. E. SALJE AND B. GUTTLER, *Philos. Mag. B* **50,** 607 (1984).
7. E. IGUCHI, *J. Phys. Chem. Solids* **38,** 1093 (1977).

8. E. IGUCHI, *J. Solid State Chem.* **23,** 231 (1978).
9. E. IGUCHI AND R. J. D. TILLEY, *J. Solid State Chem.* **24,** 131 (1978).
10. E. IGUCHI AND R. J. D. TILLEY, *J. Solid State Chem.* **29,** 435 (1979).
11. D. C. DIENES, D. O. WELCH, C. R. FISCHER, R. D. HATCHER, O. LAZARETH, AND M. SAMBERG, *Phys. Rev. B* **11,** 3060 (1975).
12. H. SAWATARI, E. IGUCHI, AND R. J. D. TILLEY, *J. Phys. Chem. Solids* **43,** 1147 (1982).
13. K. AIZAWA, E. IGUCHI, AND R. J. D. TILLEY, *Proc. R. Soc. Lond. A* **394,** 299 (1984).
14. P. W. ANDERSON, *Phys. Rev. Lett.* **34,** 853 (1975).
15. E. IGUCHI AND T. YAMAMOTO, *J. Phys. Chem. Solids* **49,** 205 (1988).
16. P. P. EWALD, *Ann. Physik.* **64,** 253 (1921).
17. W. VAN GOOL AND A. G. PIKEN, *J. Mater. Sci.* **4,** 95 (1969).
18. C. R. A. CATLOW, J. PHYS. C; *Solid State Phys.* **6,** L64 (1973).
19. M. P. TOSI, *in* "Solid State Physics" (F. Seiyz and D. Turnbull, Eds.), Vol. 16, p. 1, Academic Press, New York (1964).
20. E. IGUCHI, T. MATSUDA AND R. J. D. TILLEY, *J. Phys. C: Solid State Phys.*, **17,** 319 (1984).
21. R. W. WYCKOFF, Crystal Structures 1, p. xxx. Interscience, N.Y. (1963).
22. S. TANISAKI, *J. Phys. Soc. Japan* **15,** 573 (1960).
23. B. O. LOOPSTRA AND P. BOLDRINI, *Acta Crystallogr.* **21,** 158 (1966).
24. B. O. LOOPSTRA AND H. M. RIETVELD, *Acta Crystallogr. Sect B* **25,** 1420 (1966).
25. P. T. WEDEPOHL, *Proc. Phys. Soc.* **92,** 79 (1967).
26. P. T. WEDEPOHL, *J. Phys. C: Solid State Phys.*, **10,** 1855 (1977).
27. P. T. WEDEPOHL, *J. Phys. C: Solid State Phys.* **10,** 1865 (1977).
28. E. IGUCHI, K. OHTAKE, T. YAMAMOTO, AND H. NISHIKAWA, *J. Nucl. Mater.* **169,** 55 (1989).
29. E. IGUCHI AND Y. YONEZAWA, *J. Phys. Chem. Solids* **51,** 313 (1990).
30. R. E. WATSON, *Phys. Rev.* **111,** 1108 (1958).
31. F. HERMANN AND S. SKILLMAN, "Atomic Structure Calculations," Prentice Hall, Englewood Cliff, NJ (1963).
32. D. R. HATREE AND W. HATREE, *Proc. R. Soc. London A* **166,** 450 (1938).
33. E. CLEMENTI AND C. ROETTI, *Atomic Nucl. Data Tables,* **14,** 177 (1974).
34. R. A. PARKER, *Phys. Rev.* **124,** 1713 (1961).
35. E. SALJE, private communication (1983).
36. A. R. RUFFA, *Phys. Rev.* **130,** 1412 (1963).
37. A. M. MOFFA, *Phys. Rev. A* **133,** 1418 (1964).
38. S. TRIEBWASSER, *J. Phys. Chem. Solids* **3,** 53 (1957).
39. K. KIRKWOOD, *Physikal Z.* **33,** 57 (1970).
40. I. M. BOSWARVA, *Phys. Rev., B* **1,** 1698 (1970).
41. S. CANTOR, *J. Chem. Phys.* **59,** 5189 (1973).
42. V. P. RYCHKOV, *Z. Oberschles. Khim.* **49,** 2161 (1979).
43. P. J. WACKMAN, W. M. HIRTHE, AND R. E. FROUNTELKAS, *J. Phys. Chem. Solids* **28,** 1525 (1967).
44. A. J. BELOVO, H. R. SHANKS, P. H. SIDDLES, AND G. C. DANIELSON, *Phys. Rev. B* **9,** 3220 (1974).
45. M. J. L. SANGSTER AND A. M. STONEHAM, *Philos. Mag.* **43,** 598 (1981).
46. E. IGUCHI AND F. MATSUSHIMA, *J. Mater. Sci.* **21,** 1046 (1967).
47. R. C. WEAST AND M. J. ASTLE, CRC Handbook of Chemistry and Physics, 63rd ed., D-34 (1982/1983), CRC press, Boca Raton, Florida.
48. M. W. ZEMANNSKY, "American Institute of Physics Handbook," 3rd ed., pp. 4–247, McGraw-Hill, NY (1969).
49. T. L. COTRELL, "The Structure of Chemical Bonds," p. 1, Academic Press, NY (1954).
50. D. R. STULL, "JANAF Thermochemical Table, p. 1, Dow Chemical Co. Midland (1965).
51. T. SHERMAN, *Chem. Rev.* **10,** 93 (1932).
52. M. F. LADD AND W. H. LEE, *Acta. Crystallogr.* **13,** 959 (1960).
53. M. L. HIGGINS AND Y. SAKAMOTO, *J. Phys. Soc. Japan* **21,** 24 (1957).
54. R. D. SHANNON AND C. T. PREWITT, *Acta Crystallogr. B* **26,** 1046 (1970).
55. A. N. CORMACK, R. M. JONES, P. W. TASKER AND C. R. A. CATLOW, *J. Solid State Chem.* **44,** 174 (1982).
56. J. C. NEWTONE-HOWES AND A. N. CORMACK, *J. Solid State Chem.* **79,** 12 (1989).
57. E. SALJE, *Ferroelectrics* **12,** 215 (1976).